Clustering effects in a microscopic four-α description of the $\alpha+{}^{12}$C system

P. Descouvemont
Physique Nucléaire Théorique et Physique Mathématique, Université Libre de Bruxelles, Campus Plaine, Code Postal 229-B1050 Bruxelles, Belgium
(Received 26 December 1990)

The $\alpha+{}^{12}$C system is investigated in the generator coordinate method, where the ^{12}C nucleus is described by three α particles located on the apexes of an equilateral triangle. The ^{12}C wave functions are projected out on the 0^+ and 2^+ states. By modifying the size of the triangle, we analyze the importance of clustering effects in ^{12}C on ^{16}O bound states, and on $\alpha+{}^{12}$C phase shifts. These effects are found to be reduced when the total spin of the $\alpha+{}^{12}$C system increases. The coupling between the $\alpha+{}^{12}$C(0^+) and $\alpha+{}^{12}$C(2^+) channels also decreases when α clustering is introduced in ^{12}C. We obtain high-energy resonances in the $\alpha+{}^{12}$C scattering. These resonances, located between 15 and 30 MeV in the center of mass, are suggested to be Pauli resonances, analog to the well-known forbidden states in the two-cluster model.

I. INTRODUCTION

Many experimental data have been obtained concerning the $\alpha+{}^{12}$C system. Elastic and inelastic cross sections have been known for many years.[1] In addition, the ^{12}C$(\alpha,\gamma)^{16}$O capture reaction plays a crucial role in nuclear astrophysics.[2] The theoretical study of the $\alpha+{}^{12}$C system raises several problems, essentially because the ^{16}O nucleus presents simultaneously one-center states such as the ground state or the 3_1^- excited state and cluster states such as the states of the well-known 0^+ and 0^- bands built on the 6.00- and 9.63-MeV states, respectively. A nonmicroscopic cluster model has been used by Buck and co-workers[3,4] to study several ^{16}O states. However, shell-model-like states, such as the ground state, are missing. Suzuki and co-workers[5,6] have investigated bound-state properties of ^{16}O and $\alpha+{}^{12}$C scattering in the orthogonality condition model (OCM). This model takes partly account of the Pauli principle, but contains several adjustable parameters. Microscopic single-channel studies of the $\alpha+{}^{12}$C system have been performed by Horiuchi,[7] Hüsken,[8] and Baye and Heenen[9] in a two-cluster $\alpha+{}^{12}$C(0^+) model. An extension has been carried out by Libert-Heinemann *et al.*[10] who include the $\alpha+{}^{12}$C$(0^+,2^+)$ channels. However, this study met a problem with the ^{12}C(2^+) excitation energy, which was underestimated. In 1987, we improved this previous work by introducing a spin-orbit force, and by taking account of the $p+{}^{15}$N and $n+{}^{15}$O configurations.[11]

Until now, all the microscopic studies of the $\alpha+{}^{12}$C system have a common drawback: with conventional nucleon-nucleon forces, the binding energy of ^{16}O with respect to the $\alpha+{}^{12}$C threshold is much larger than the experimental value (-7.16 MeV). This is due to the fact that the α and ^{16}O nuclei are well described in the one-center harmonic-oscillator model, whereas ^{12}C is not. Fujiwara and coworkers[12] have shown that the ^{12}C wave function can be significantly improved by using a triple-α model. In this paper, we present a microscopic study of the $\alpha+{}^{12}$C system, where ^{12}C is described by three α particles located on the apexes of an equilateral triangle. This model is expected to provide a more reliable description for the $\alpha+{}^{12}$C system; in particular, it should reduce the disagreement observed for the ^{16}O binding energy in two-center microscopic models. Moreover, it allows one to analyze the influence of clustering effects in ^{12}C on the ^{16}O spectrum and on the $\alpha+{}^{12}$C phase shifts. Note, however, that a four-α model raises important numerical problems since the ^{12}C wave functions have to be projected out on spin and parity in order to have a physical description of the $\alpha+{}^{12}$C scattering. Our aim in the present work is not a comparison with experiment. We only want to investigate qualitatively the effects of the ^{12}C deformation on the $\alpha+{}^{12}$C system by varying the size of the triangle.

II. THE MICROSCOPIC FOUR-α MODEL

In a microscopic model, the wave functions are antisymmetrized with respect to the exchange of all the nucleons. They can be projected out on the good quantum numbers of the system.[13] Let $\phi^{I\nu}_{C,K}(R_C)$ be a ^{12}C wave function with spin I, projection ν, and intrinsic projection K. This nucleus is assumed to be described by three α clusters located on the apexes of an equilateral triangle with side R_C (see Fig. 1). The symmetry of the equilateral triangle leads to a strong reduction of computer times. In addition, as far as we are concerned with the ground-state band of ^{12}C, the validity of this approximation is supported by the sharp minimum of the binding energy around an equilateral triangle.[12] With this configuration, one has $K=3n$, where n is a positive integer number, and the parity is given by $(-)^K$. We have

$$\phi^{I\nu}_{C,K}(R_C)=\phi^{-1}_{\text{c.m.}}\int D^{I*}_{\nu K}(\Omega)\mathcal{R}(\Omega)\mathcal{A}\Phi_\alpha(\mathbf{S}_1)\times\Phi_\alpha(\mathbf{S}_2)\Phi_\alpha(\mathbf{S}_3)d\Omega \quad (1)$$

where $\phi_{\text{c.m.}}$ is a center-of-mass function, $D^I_{\nu K}(\Omega)$ and $\mathcal{R}(\Omega)$ are the Wigner function and the rotation operator, depending on the Euler angles Ω. Owing to the symme-

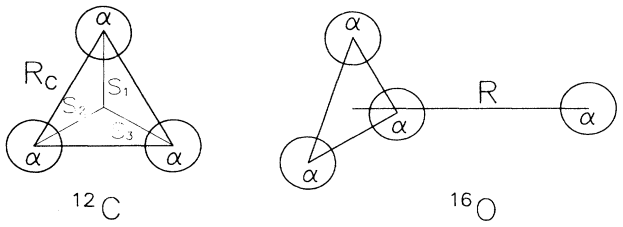

FIG. 1. Cluster structure of ^{12}C and ^{16}O in the present model.

try of the system, the integration domain can be reduced, yielding a significant reduction of the calculation times. In (1), $\Phi_\alpha(\mathbf{S}_i)$ is a Slater determinant relative to the α particle and defined in the harmonic-oscillator model with parameter b; it is composed of four s orbitals centered at S_i, which depends on R_C and on the Euler angles (see Fig. 1). The antisymmetrization of the wave function is ensured by the operator $\mathcal{A}$. Note that when R_C tends towards zero in (1), one obtains the usual one-center description of ^{12}C. In this approximation, the ^{12}C basis wave functions are determined in order to have good spin and parity, without additional projection. This description has been used by previous authors[7–10] in two-center microscopic studies of $\alpha+^{12}C$ scattering. The originality of the present work is to allow the R_C value to be different from zero. As it is well known,[12] this procedure improves the ^{12}C wave functions and, consequently, the study of the $\alpha+^{12}C$ scattering is expected to be more reliable.

In an $\alpha+^{12}C$ model, an ^{16}O wave function where ^{12}C is described by an equilateral triangle with side R_C reads

$$\Psi^{JM\pi}(R_C)=\mathcal{A}\sum_{lI}\phi_\alpha[Y_l(\hat{\rho})\otimes\phi_C^I(R_C)]^{JM}g_{lI}^{J\pi}(\rho,R_C) \quad (2)$$

where ρ is the relative coordinate between α and ^{12}C, and l is the angular momentum. Up to a center-of-mass factor, the internal wave function ϕ_α is equivalent to the Slater determinant Φ_α. According to the high excitation energy of the $^{12}C(3^-)$ state, we neglect the $K=3$ configuration, and we restrict ourselves to $K=0$. Therefore, we drop this index in the ^{12}C wave functions. Function $g_{lI}^{J\pi}(\rho,R_C)$ is a radial wave function determined from the ^{16}O Hamiltonian. In the Generator Coordinate Method (GCM), this function is expanded as projected Gaussian functions[14] $\Gamma_l(\rho,R)$, yielding

$$g_{lI}^{J\pi}(\rho,R_C)=\int f_{lI}(R,R_C)\Gamma_l(\rho,R)dR \ , \quad (3)$$

where R is the generator coordinate associated to the $\alpha+^{12}C$ relative motion (see Fig. 1), and $f_{lI}^{J\pi}$ the weight function. Before inserting (3) in (2), let us define a four-alpha determinant:

$$\Phi_{4\alpha}(\mathbf{R},R_C,\Omega)=\mathcal{A}\Phi_\alpha(-\tfrac{1}{4}\mathbf{R}+\mathbf{S}_1)\Phi_\alpha(-\tfrac{1}{4}\mathbf{R}+\mathbf{S}_2)\times\Phi_\alpha(-\tfrac{1}{4}\mathbf{R}+\mathbf{S}_3)\Phi_\alpha(\tfrac{3}{4}\mathbf{R}) \ . \quad (4)$$

Now, using (1) to (4), we find

$$\Psi^{JM\pi}(R_C)=\sum_{lI}\int f_{lI}^{J\pi}(R,R_C)\Phi_{lI}^{JM\pi}(R,R_C)dR \ , \quad (5)$$

where

$$\Phi_{lI}^{JM\pi}(R,R_C)=\sum_\nu\langle lIM-\nu\nu|JM\rangle\times\int Y_l^{M-\nu*}(\hat{\mathbf{R}})D_{\nu0}^{I*}(\Omega)\times\Phi_{4\alpha}(\mathbf{R},R_C,\Omega)d\hat{R}\,d\Omega \ . \quad (6)$$

The weight function $f_{lI}^{J\pi}(R,R_C)$ and the relative function $g_{lI}^{J\pi}(\rho,R_C)$ can be obtained from the matrix elements of the overlap and of the Hamiltonian between projected Slater determinants (6). A straightforward calculation leads to

$$\langle\Phi_{lI}^{J\pi}(R,R_C)|H|\Phi_{l'I'}^{J\pi}(R',R_C')\rangle=8\pi^2\sum_\nu\langle lIM-\nu\nu|JM\rangle\sum_{\nu'}\langle l'I'M'-\nu'\nu'|JM\rangle\times\int Y_l^{M-\nu}(0,0)D_{\nu,0}^{I}(\Omega)Y_{l'}^{M-\nu'*}(\theta,0)D_{\nu',0}^{I'*}(\Omega')\times\langle\Phi_{4\alpha}(\mathbf{R},R_C,\Omega)|H|\Phi_{4\alpha}(\mathbf{R}',R_C',\Omega')\rangle d\theta\,d\Omega\,d\Omega' \ , \quad (7)$$

where $\mathbf{R}$ is along the z axis, and $\mathbf{R}'$ makes an angle θ with respect to $\mathbf{R}$, and is located in the x-z plane. Expression (7) shows that the matrix elements depend upon seven-dimensional integrals. This result raises tremendous numerical problems and requires the access to a supercomputer. Most of the computer time is devoted to the matrix elements of the two-body force between Slater determinants (4). However, since the four clusters are here α particles, this calculation can be efficiently optimized. In addition, the quadrupole sums involved in these matrix elements can be highly vectorized.

III. CONDITIONS OF THE CALCULATION

The Hamiltonian contains the $V2$ nucleon-nucleon force,[15] and the exact Coulomb interaction. In an alpha-cluster model, the spin-orbit and tensor forces do not contribute to the matrix elements. The oscillator parameter is chosen as $b=1.36$ fm, which minimizes the binding energy of the α particle. We shall consider four approaches, with different R_C values (0.4, 1.6, 2.8, 4.0 fm). The value $R_C=0.4$ fm nearly corresponds to a one-center description of ^{12}C, and $R_C=2.8$ fm represents the minimum of the expectation value of the Hamiltonian with the standard Majorana parameter $M=0.6$. Two additional values are selected in order to analyze the importance of α clustering in $^{12}C(R_C=1.6$ and 4.0 fm). The $\alpha+^{12}C(0^+,2^+)$ channels are included in the calculation. We have performed a few simplified calculations (i.e., with a single set of generator coordinates) involving the $\alpha+^{12}C(4^+)$ configuration. For low-lying ^{16}O states, this

channel plays a negligible role, and therefore is not taken into account. The generator coordinates R between α and ^{12}C are selected from 1.1 to 8.8 fm with a step of 1.1 fm. The Majorana parameter is adjusted in order to reproduce the energy of the 0_2^+ and 1_1^- states in ^{16}O, in positive and negative parity, respectively, with $R_C=2.8$ fm. This leads to $M=0.644$ in positive parity and $M=0.650$ in negative parity. These values are used in the four calculations involving the different R_C generator coordinates. They are not the best choices when R_C is different from 2.8 fm. However, in order to provide a meaningful analysis of clustering effects, it is necessary to use the same interaction when R_C varies.

In Fig. 2, we present the expectation value of the ^{12}C Hamiltonian ($M=0.644$) with respect to R_C. As it is well known,[12] the binding energy significantly increases when R_C is allowed to be different from zero. The minimum is obtained here at 3.1 fm and the 2^+ excitation energy is 3.11 MeV. This result is smaller than the experimental value[16] (4.44 MeV) but improves the one-center excitation energy (1.27 MeV). Let us notice that, with our choice of the Majorana parameter, the absolute binding energy of ^{12}C, and therefore of ^{16}O, does not reproduce the experimental value. The present ^{12}C description reduces this problem with respect to the one-center approximation, where much higher values of the Majorana parameter are required[10] to reproduce the $\alpha+^{12}C$ threshold in ^{16}O. However, a more precise description of the absolute ^{12}C and ^{16}O energies simultaneously remains an open problem.

In Table I, we present different spectroscopic properties of ^{12}C as a function of R_C. This table confirms that using an R_C value close to 3 fm is necessary to reproduce the experimental rms radius of the ground state, the 2^+ quadrupole moment, as well as the $B(E2,2^+\rightarrow 0^+)$ value. However, the excitation energy of the 2^+ state remains somewhat underestimated, even with large R_C values.

In the following, the microscopic R-matrix method (MRM) is used to calculate the bound-state and resonance energies as well as the collision matrices. The MRM radius a is chosen as $a=7.7$ fm. We refer the reader to Refs. 14 and 17 for details concerning the MRM.

IV. THE $\alpha+^{12}C$ SYSTEM

A. Energy curves

For each R_C value, the energy curves $E_{lI}^{J\pi}(R,R_C)$ are defined as

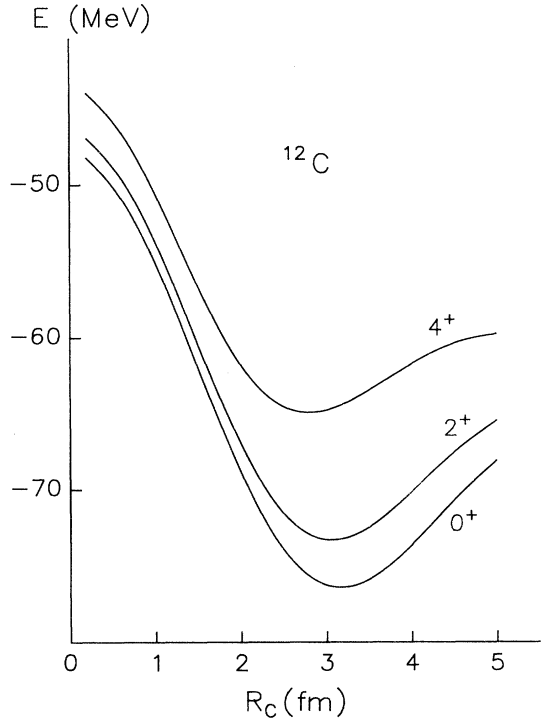

FIG. 2. Binding energy of the 0^+, 2^+, and 4^+ states of ^{12}C as a function of R_C.

$$E_{lI}^{J\pi}(R,R_C)=\frac{\langle\Phi_{lI}^{J\pi}(R,R_C)|H|\Phi_{lI}^{J\pi}(R,R_C)\rangle}{\langle\Phi_{lI}^{J\pi}(R,R_C)|\Phi_{lI}^{J\pi}(R,R_C)\rangle} . \quad (8)$$

The energy curves must not be considered as nucleus-nucleus potentials, but they provide a qualitative information about this interaction.[18] Let us first consider the $\alpha+^{12}C(0^+)$ single-channel system ($I=0$, $l=J$). The energy curves are presented in Fig. 3 for positive-parity partial waves, and in Fig. 4 for negative-parity partial waves. The minimum of the 0^+ energy curves can be associated to the ^{16}O ground state. The location of this minimum weakly depends on R_C, and the binding energy of ^{16}O is much less affected by R_C than the binding energy of ^{12}C. Therefore, if the ^{16}O energy with respect to the $\alpha+^{12}C$ threshold is strongly overestimated with small R_C values, it is expected to be reduced when R_C increases. For J larger than 0, the positive-parity energy curves are nearly parallel, but for $J^\pi=2^+$, the location of the minimum is pushed up to higher values of the generator coordinate R

TABLE I. ^{12}C properties with different R_C values.

	0.4 fm	1.6 fm	2.8 fm	4.0 fm	Expt. (Ref. 16)
$E(2^+)-E(0^+)$ (MeV)	1.28	1.51	2.75	3.52	4.44
$\sqrt{\langle r^2\rangle_{0+}}$ (fm)	1.95	2.06	2.34	2.88	2.48
Q_{2+} (e fm^2)	2.95	3.70	5.71	9.67	6±3
$B(E2,2^+\rightarrow 0^+)$ (e^2 fm^4)	1.97	3.23	8.23	23.7	7.8±0.4

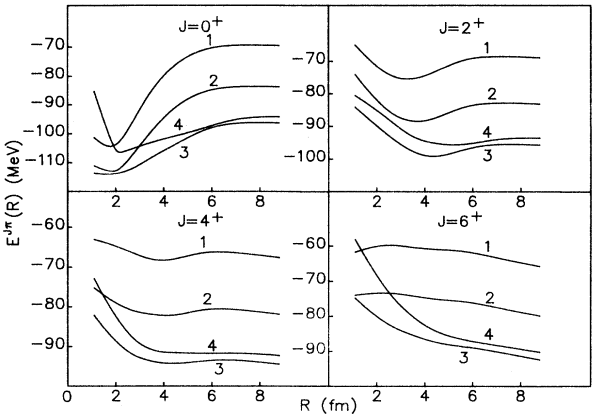

FIG. 3. $\alpha+{}^{12}C(0^+)$ energy curves in positive parity [see Eq. (8)]. The labels 1, 2, 3, and 4 correspond to $R_C=0.4$, 1.6, 2.8, and 4.0 fm, respectively.

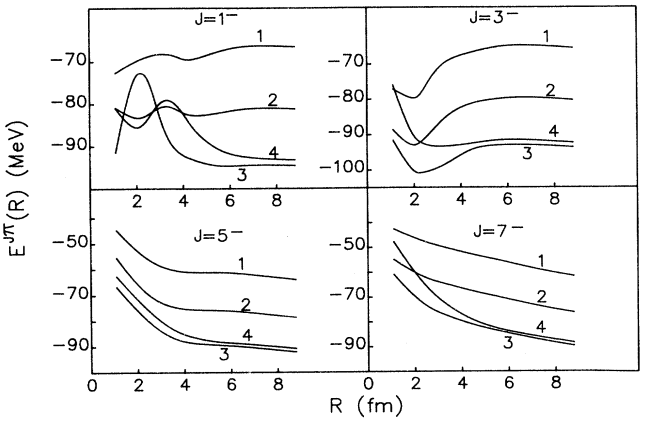

FIG. 4. As in Fig. 3 but for negative parity.

when going from $R_C=0.4$ to 4.0 fm. The $\alpha+{}^{12}C$ clustering in the 2_1^+ bound state of ^{16}O is therefore expected to be stronger with a three-cluster description of ^{12}C than with a one-center approximation. For $J^\pi=4^+$ and 6^+, the repulsion at small generator coordinates increases for large values of R_C.

Let us now discuss the negative-parity energy curves displayed in Fig. 4. For $J^\pi=1^-$, the energy curves relative to $R_C=2.8$ and 4.0 fm present a striking property. The Coulomb barrier almost disappears, and is replaced by a bump near 2.1 and 3.2 fm. In fact, if the ^{16}O nucleus is assumed to be described by a symmetric four α tetrahedral configuration, a 1^- spin is forbidden. In the present model, the configuration is not rigid since ^{12}C is projected on spin and parity, but the location of the bumps nearly corresponds to this situation since we have $R\approx\frac{3}{4}R_C$. For $J^\pi\geq 3^-$, the energy curves are nearly equidistant except for the $R_C=4.0$ fm curves which are slightly more repulsive at small R values. Accordingly, from the energy curves, the influence of clustering effects in the ^{12}C description is expected to decrease with increasing J values. In this case, the difference between the energy curves essentially arises from the ^{12}C binding energies.

When the $\alpha+{}^{12}C(2^+)$ channel is taken into account, it is useful to define a new basis which diagonalizes the Hamiltonian for each set of (R,R_C) values.[19] This provides the energy surfaces $E_\omega^{J\pi}(R,R_C)$ given by

$$\sum_{l'I'}\langle\Phi_{lI}^{J\pi}(R,R_C)|H-E_\omega^{J\pi}(R,R_C)|\Phi_{l'I'}^{J\pi}(R,R_C)\rangle d_{\omega,l'I'}^{J\pi}(R,R_C)=0 \tag{9}$$

where $\mathbf{d}^{J\pi}(R,R_C)$ is the matrix of the transformation and ω is the level of excitation in the relative motion. The number of ω values is equal to the number of (lI) values. The advantage of this basis is to separate the multichannel problem in different single-channel approaches.[19] In Fig. 5, we present the 0^+ energy surfaces for $\omega=1$ and $\omega=2$. The energy scale is arbitrary, and the shift between the $\omega=1$ and $\omega=2$ energy surfaces has been increased for the sake of clarity. For $\omega=1$, the minimum is located near $R=2.0$ fm and $R_C=2.7$ fm. This can be roughly interpreted as a symmetric tetrahedral configuration since $R\approx\frac{3}{4}R_C$. Figure 5 confirms that the influence of ^{12}C clustering is much more important at large R values than at small R values. In the $\omega=2$ energy surface, the introduction of clustering in ^{12}C enhances the binding energy. The minimum is located near $R=4.4$ fm and $R_C=3.3$ fm. In the 1^- energy surfaces displayed in Fig. 6, the bump obtained in the $\alpha+{}^{12}C$ (0^+) single-channel approximation (see Fig. 4) is no longer present, since ^{12}C can now be excited. There is a minimum near $R=4.2$ fm and $R_C=2.8$ fm in the $\omega=1$ surface. For $\omega=2$ and $\omega=3$, clustering effects are more important ($R\approx 5$ fm, $R_C\approx 3.2$ fm at the minimum).

B. ^{16}O spectra

The GCM ^{16}O spectra calculated with the $\alpha+{}^{12}C(0^+)$ configuration alone are presented in Fig. 7. For the sake of clarity, the absolute energies are displayed; we also give in dotted lines the $\alpha+{}^{12}C$ thresholds. For the experimental spectrum, we take the GCM threshold obtained with $R_C=2.8$ fm. Figure 7 shows that the binding energies of ^{16}O states are less affected by α clustering than the ^{12}C states. For almost all states, the energies with respect to the $\alpha+{}^{12}C$ threshold increase with the generator coordinate R_C. This is especially true for the ground state. At $R_C=0.4$ fm, the binding energy is -28.2 MeV, which becomes -12.7 MeV at $R_C=2.8$ fm. This binding energy remains larger than the experimental value (-7.16 MeV) but the improvement is significant. For the 4^+ state, on the contrary, the energy with respect to the $\alpha+{}^{12}C$ threshold is nearly insensitive to the ^{12}C deforma-

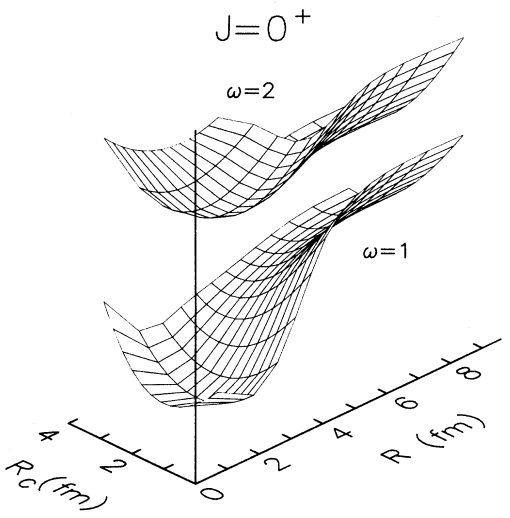

FIG. 5. $\alpha+^{12}C(0^+,2^+)$ energy surfaces for $J^\pi=0^+$.

tion. This supports the interpretation of the energy curves which predict that clustering effects are weaker when J increases.

The corresponding spectra with the $\alpha+^{12}C(0^+,2^+)$ configurations are shown in Fig. 8. The theoretical $\alpha+^{12}C(2^+)$ thresholds are also presented. The comparison of Figs. 7 and 8 indicates that the coupling between the $\alpha+^{12}C(0^+)$ and $\alpha+^{12}C(2^+)$ channels is more and more important when R_C decreases. This is especially obvious for the ground state. For $R_C=0.4$ fm, the ordering of the 0_2^+ and 2_1^+ states, which are well known to be members of a same rotational band, is even incorrect. The physical order, with a reasonable spacing between both states, is restored for $R_C=2.8$ fm. An other interesting property is the energy difference between the 1_2^- and 1_1^- states. The spacing is largely overestimated with

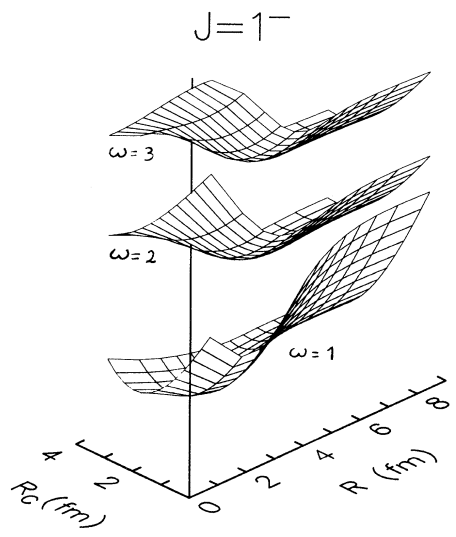

FIG. 6. $\alpha+^{12}C(0^+,2^+)$ energy surfaces for $J^\pi=1^-$.

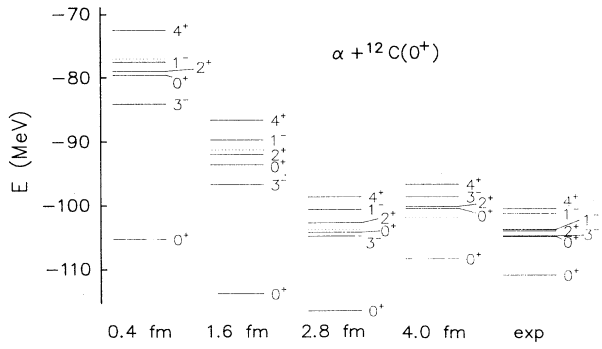

FIG. 7. ^{16}O spectra in the $\alpha+^{12}C(0^+)$ model for different R_C values. The $\alpha+^{12}C$ thresholds are represented by dotted lines.

small R_C values; with $R_C=0.4$ fm we obtain an energy difference of 11.8 MeV. For $R_C=2.8$ fm, we get a spacing of 3.6 MeV, in a reasonable agreement with experiment (2.47 MeV) if one keeps in mind that the 1_2^- resonance has most likely an important component in the $p+^{15}N$ and $n+^{15}O$ channels.[11]

In order to analyze more deeply the influence of clustering effects in ^{12}C, we give in Table II the rms radius of the ^{16}O ground state, and the mean distance d between α and ^{12}C for different states. The mean distance d is obtained from the rms radii of ^{16}O, ^{12}C, and α by

$$3d^2=16\langle r^2\rangle_O-12\langle r^2\rangle_C-4\langle r^2\rangle_\alpha \ . \tag{10}$$

The rms radii of ^{12}C are given in Sec. III; for the α particle, we use the shell-model value ($\langle r^2\rangle_\alpha=9b^2/8$). The ^{16}O rms radii are calculated with the wave functions (5). Let us first discuss the ground-state rms radius. For $R_C=0.4$ fm, we obtain a value close to the shell-model approximation ($\sqrt{\langle r^2\rangle}=b\sqrt{69/32}=2.00$ fm). This result confirms that, for small values of R_C, the clustering between ^{12}C and α is negligible in the ground state. Except for $R_C=4.0$ fm, the $\alpha+^{12}C(2^+)$ configuration increases the rms radius. The experimental value ($\sqrt{\langle r^2\rangle}=2.70$ fm) would correspond to R_C between 2.8 and 4.0 fm. For the 0_2^+ and 2_1^+ states, which are believed

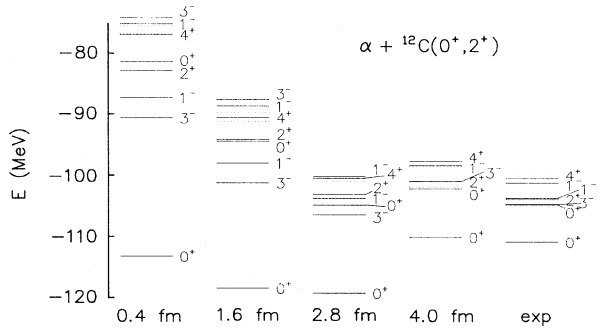

FIG. 8. ^{16}O spectra in the $\alpha+^{12}C(0^+,2^+)$ model for different R_C values. The $\alpha+^{12}C(0^+)$ and $\alpha+^{12}C(2^+)$ thresholds are represented by dotted lines.

TABLE II. rms radius and mean distances d in ^{16}O.

J^π	R_C=0.4 fm (a)	(b)	1.6 fm (a)	(b)	2.8 fm (a)	(b)	4.0 fm (a)	(b)
				$\sqrt{\langle r^2\rangle}$				
0_1^+	2.10	2.17	2.19	2.26	2.40	2.51	2.87	2.82
				d				
0_1^+	2.35	2.67	2.14	2.74	2.46	2.51	2.82	2.54
0_2^+ [c]	3.88	3.50	4.00	3.65	4.73	4.53	5.73	4.78
0_2^+ [d]	4.15	3.99	4.24	4.07	4.60	4.53	4.89	4.55
2_1^+	3.73	3.31	4.07	3.58	4.86	4.73	5.45	4.89
1_1^-	4.76	2.96	5.46	3.19	5.87	3.65		4.89
3_1^-	2.53	2.80	2.65	2.95	2.99	3.21	3.74	3.42

[a]Single-channel calculation.
[b]Multichannel calculation.
[c]M=0.644.
[d]M adjusted to the experimental energy (see text).

to be $\alpha+^{12}$C cluster states,[5] we find that, not only $\sqrt{\langle r^2\rangle}$, but also d increases with R_C. Since this effect might be partly due to the binding energy with respect to the $\alpha+^{12}$C channel, we have carried out a calculation where the Majorana parameter is adjusted, for each R_C value and choice of configuration, to reproduce the experimental binding energy of the 0_2^+ state (−1.11 MeV). The results obtained in this way confirm the increase of d with R_C, even with an energy correction on the wave functions. Accordingly, the rms radii in ^{16}O low-lying states are increased, not only by α clustering of ^{12}C, but also by a larger mean distance between α and ^{12}C. This conclusion remains true for the 1_1^- and 3_1^- states.

C. $\alpha+^{12}$C phase shifts

In Figs. 9 and 10, we present the $\alpha+^{12}$C elastic phase shifts in the single-channel model. At zero energy, we choose

$$\delta^{J\pi}(0)=n^{J\pi}\pi\ , \tag{11}$$

where $n^{J\pi}$ is the number of bound states in the partial wave $J\pi$. Figures 9 and 10 show that, at a given energy, the phase shifts decrease with increasing values of R_C. In positive parity, the 0^+ and 2^+ phase shifts present narrow resonances located between 15 and 20 MeV for large R_C values. The analysis of these resonances is delayed to

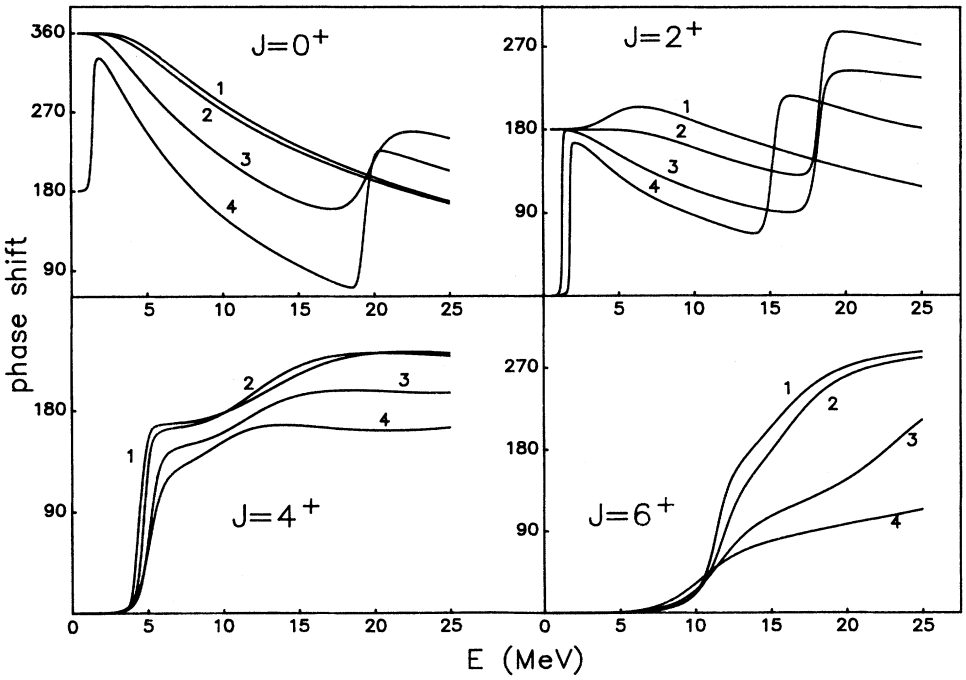

FIG. 9. Elastic $\alpha+^{12}$C phase shifts in the single-channel model for positive-parity partial waves. The curves are labeled as in Fig. 3.

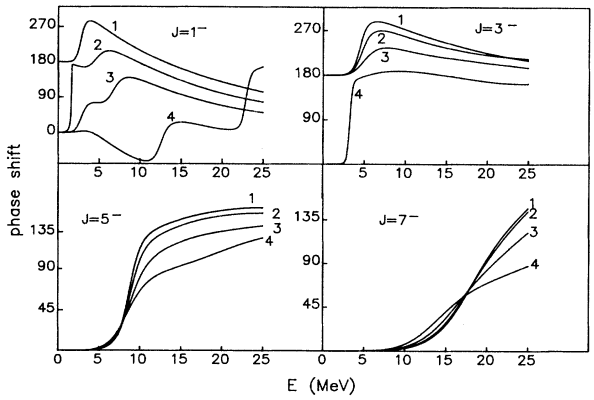

FIG. 10. See caption to Fig. 9 for negative-parity partial waves.

the next subsection. For $J^\pi=4^+$ and 6^+, the resonance energy is weakly dependent on R_C, in agreement with the conclusions drawn in Sec. IV B. The 1^- phase shift in Fig. 10 shows an additional resonance near 23 MeV for $R_C=4.0$ fm. As for the 0^+ and 2^+ partial waves, we send the reader to Sec. IV D for the study of the origin of these resonances. The 3^- phase shifts contain the well-known broad 3_2^- resonance, except for $R_C=4.0$ fm, where this resonance is pushed up to the background contribution. As already observed for $J=4^+$ and 6^+, the phase shifts relative to high negative-parity partial waves are weakly affected by the deformation of ^{12}C.

Figures 11 and 12 give information concerning the $\alpha+^{12}C(0^+,2^+)$ collision matrices $U^{J\pi}_{l,l',I'}$. They are parametrized as

$$U^{J\pi}_{l,l',I'}=\eta^{J\pi}_{l,l'I'}\exp(2i\delta^{J\pi}_{l,l'I'}) . \quad (12)$$

The lower parts of the figures contain the elastic phase shifts $\delta^{J\pi}_{J0,J0}$ whereas the upper parts give the amplitudes $\eta^{J\pi}_{J0,J0}$. In both parities, the conclusions are similar. At low spin, the differences in the shapes of the phase shifts are reduced with respect to the single-channel calculation. High-energy resonances appear in the 0^+ phase shift for $R_C=2.8$ fm and $R_C=4.0$ fm, and in the 1^- phase shift for $R_C=4.0$ fm. In addition, the absorption in the $\alpha+^{12}C(2^+)$ channel decreases with increasing values of R_C. This confirms the conclusion drawn in the study of ^{16}O spectra which states that the coupling between the $\alpha+^{12}C(0^+)$ and $\alpha+^{12}C(2^+)$ channels is the most important at small R_C values. The 0^+ phase shift presents a narrow resonance assigned to the 12.05-MeV state in ^{16}O [for $R_C=4.0$ fm, this resonance is observed in the $\alpha+^{12}C(2^+)$ channel]. At high spin, the influence of R_C is much weaker, except above 20 MeV in the 7^- collision matrix.

D. Pauli forbidden states

In microscopic descriptions of single-channel elastic scattering, it is well known that the Swan generalization[20] of the Levinson theorem leads to

$$\delta^{J\pi}(E=0)-\delta^{J\pi}(E=\infty)=(n^{J\pi}+m^{J\pi})\pi \quad (13)$$

where $n^{J\pi}$ is the number of bound states, and $m^{J\pi}$ the number of Paul forbidden states. The occurrence of forbidden states thus provides a strong constraint on the energy dependence of the phase shift. When both colliding nuclei are described in the one-center harmonic-oscillator

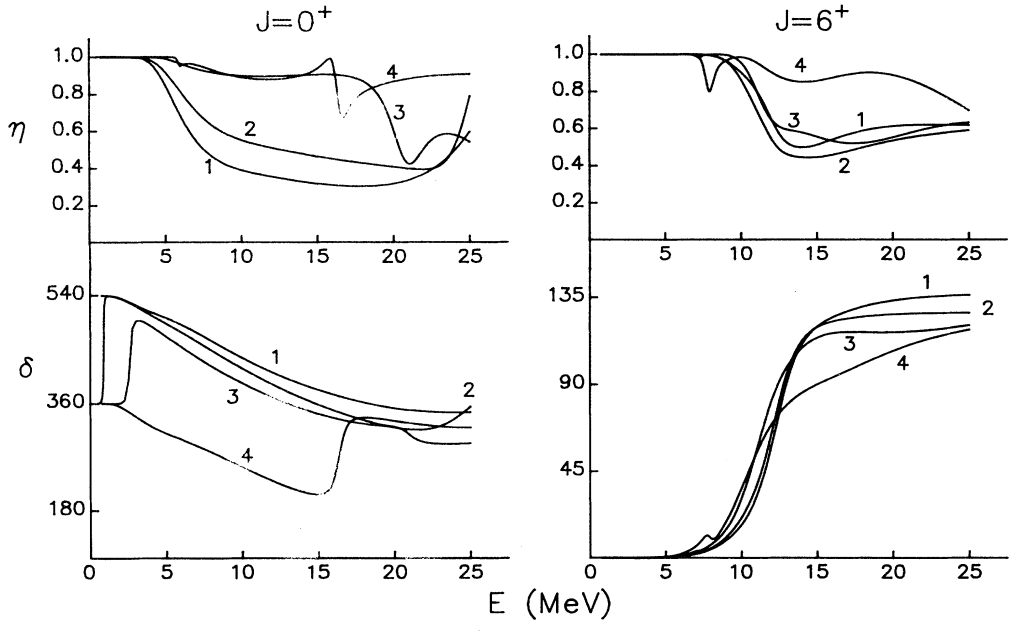

FIG. 11. Elastic phase shifts $\delta^{J\pi}_{J0,J0}$ and absorption coefficients $\eta^{J\pi}_{J0,J0}$ [see Eq. (12)] in the $\alpha+^{12}C(0^+,2^+)$ model for $J^\pi=0^+$ and 6^+. The curves are labeled as in Fig. 3.

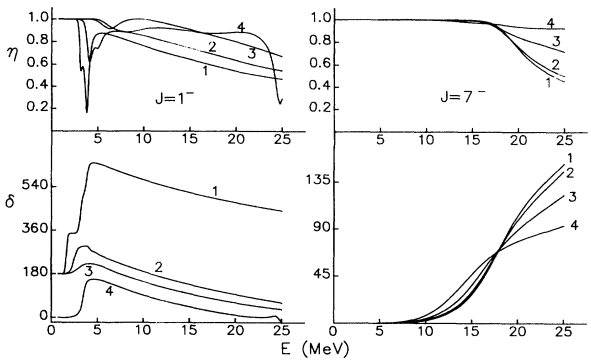

FIG. 12. As in Fig. 11 but for $J^{\pi}=1^{-}$ and 7^{-}.

model with a common oscillator parameter, the forbidden states arise from the fact that, when the distance between both clusters tends towards zero, the wave function vanishes if a single-particle orbital is occupied twice. However, if at least one of the colliding nuclei is described by a multicluster configuration, this property does not remain true. Accordingly, at first sight, forbidden states are removed, and the energy dependence of the phase shifts should be strongly modified when going from a one-center description to a three-α description of ^{12}C.

In fact, the phase shifts presented in Figs. 9 and 10 suggest that the role of the forbidden states is played by high-energy resonances. These resonances might be related to the resonances observed in the two-center nucleus-nucleus scattering with different oscillator parameters[21] and probably are the analogs of the Pauli resonances. At low energy, the phase shifts are not much affected by these resonances, but, when the energy increases, the phase shifts are increased by about 180°. Consequently, except in the nearby vicinity of these resonances, elastic-scattering cross sections would not be very different when R_C varies. In Table III, we give the energy and width of high-energy resonances in the 0^+, 2^+, and 1^- partial waves. If the analogy with Pauli forbidden states is meaningful, their number is expected to be equal to the number of forbidden states in a two-center description of $\alpha+^{12}$C scattering (i.e., $m^{0^+}=2$, $m^{2^+}=2$, $m^{1^-}=2$). However, the second Pauli resonance is most likely located at very high energy, where our phase shifts would not be numerically accurate enough. Table III shows that the energy as well as the width of these resonances decrease when R_C increases. This is because the influence of the Pauli principle between α and ^{12}C is lowered for large R_C values. For $R_C=0.4$ fm, Pauli resonances in $\alpha+^{12}$C(0^+) scattering are not found in the energy range considered here. When the $\alpha+^{12}$C(2^+) channel is introduced, relation (13) is no longer valid, and therefore the existence of Pauli resonances may be questioned. However, according to the single-channel study, such resonances are expected to be rather narrow and located far above the Coulomb barrier. Consequently, high-energy resonances obtained in the $\alpha+^{12}$C(0^+,2^+) calculation might have common properties with Pauli resonances. The introduction of the $\alpha+^{12}$C(2^+) channel increases their excitation energy except for the 0^+ partial wave at $R_C=4.0$ fm. These resonances are sensitive to the number of channels and to the ^{12}C deformation. Accordingly, a more precise study of these resonances should require the combination of different R_C generator coordinates, and the introduction of other channels, such as $p+^{15}$N or $n+^{15}$O.

V. CONCLUSION

The aim of this work is a microscopic investigation of $\alpha+^{12}$C scattering with ^{12}C wave functions described in a triple-α configuration. This description significantly improves the ^{12}C wave function with respect to the one-center approximation. The binding energy is enhanced by more than 25 MeV, and the spectroscopic properties, which completely disagree with experiment in the one-center description, are in remarkable agreement when α clustering is introduced. A further advantage of the present ^{12}C description is to provide the 0^+ and 2^+ wave functions simultaneously. This model could be in principle applied to other systems involving an s-shell particle and a nucleus described by three s orbitals located on the apexes of a triangle. The main limitation of such a multicluster model is the calculation of matrix elements, which involves seven-dimensional integrals. In the present case, the presence of four-α particles, and the assumption of an equilateral triangle for ^{12}C, lead to an efficient vectorization of the computer code and make this calculation possible.

In this paper, we focus on clustering effects in $\alpha+^{12}$C scattering, but in this first step we are not concerned with

TABLE III. Energies and widths Γ_I of Pauli resonances. Lengths are expressed in fm, and energies in MeV.

	0^+			2^+			1^-		
	$E_{c.m.}$	Γ_0	Γ_2	$E_{c.m.}$	Γ_0	Γ_2	$E_{c.m.}$	Γ_0	Γ_2
				$\alpha+^{12}$C(0^+)					
1.6				18.3	0.3				
2.8	~20	~3		18.2	0.5				
4.0	19.5	0.2		15.1	0.3		22.9	0.6	
				$\alpha+^{12}$C(0^+,2^+)					
1.6	~26	~2	~1						
2.8	~21	~1	~3	~28	~2	~1			
4.0	16.3	0.6	0.1	23.4	0.5	0.6	24.5	0.2	0.9

a comparison with experiment. An extension of this work could be to introduce distortion effects in ^{16}O by combining different R_C values for the ^{12}C wave functions. In this way, the ^{16}O wave functions should be rather reliable and a comparison with experiment should be meaningful. The present model could be also applied to the $E2$ component of the $^{12}C(\alpha,\gamma)^{16}O$ cross section, which still remains uncertain.[22]

The main results are the following. The study of the ^{16}O rms radii shows that $\alpha+^{12}C$ clustering increases with the side R_C of the equilateral triangle. When R_C increases, not only the rms radius of ^{12}C becomes larger, but also the distance between the α and ^{12}C nuclei. According to the study of $\alpha+^{12}C$ phase shifts and of ^{16}O spectra, the influence of clustering in ^{12}C decreases with increasing values of J. In addition, clustering effects in ^{12}C reduce the coupling between the $\alpha+^{12}C(0^+)$ and $\alpha+^{12}C(2^+)$ channels.

The present multicluster model gives rise to high-energy narrow resonances in the $\alpha+^{12}C$ phase shifts. These resonances might be associated to the Pauli forbidden states in two-center calculations with different oscillator parameters. They are located around 20 MeV, with a width in general lower than 1 MeV, but their precise location depends on R_C and on the number of $\alpha+^{12}C$ channels. Of course, at such high energies, many other channels are open, and the properties of the high-energy resonances might be significantly affected. The introduction of excited channels, such as $p+^{15}N$ and $n+^{15}O$, should probably give a more realistic description of these resonances, and deserves further studies.

ACKNOWLEDGMENTS

I am grateful to Professor D. Baye for his careful reading of my manuscript. This work was supported by the Fonds National de la Recherche Scientifique. The numerical calculations have been carried out thanks to a supercomputer grant on the CRAY X-MP of the ULB-VUB computer center.

[1]F. Ajzenberg-Selove, Nucl. Phys. **A460**, 1 (1986).
[2]C. Rolfs, H. P. Trautvetter, and W. S. Rodney, Rep. Prog. Phys. **50**, 233 (1987).
[3]B. Buck and J. A. Rubio, J. Phys. G **10**, L209 (1984).
[4]R. A. Baldock, B. Buck, and J. A. Rubio, Nucl. Phys. **A426**, 222 (1984).
[5]Y. Suzuki, Prog. Theor. Phys. **55**, 1751 (1976); **56**, 111 (1976).
[6]Y. Suzuki, T. Ando, and B. Imanishi, Nucl. Phys. **A295**, 365 (1978).
[7]H. Horiuchi, in *Proceedings of the INS-IPCR Symposium on Cluster Structure of Nuclei and Transfer Reations Induced by Heavy Ions, Tokyo, 1975,* edited by H. Kamitsubo, I. Kohno, and T. Marumori (The Institute of Physical and Chemical Research, Wako-shi, Saitama, Japan, 1975), p. 41.
[8]H. Hüsken, Nucl. Phys. **A291**, 206 (1977).
[9]D. Baye and P.-H. Heenen, Fizika (Zagreb) **9**, Suppl. **3**, 1 (1977).
[10]M. Libert-Heinemann, D. Baye, and P.-H. Heenen, Nucl. Phys. **A339**, 429 (1980).
[11]P. Descouvemont, Nucl. Phys. **A470**, 309 (1987).
[12]Y. Fujiwara, H. Horiuchi, K. Ikeda, M. Kamimura, K. Katō, Y. Suzuki, and E. Uegaki, Prog. Theor. Phys. Suppl. **68**, 29 (1980).
[13]Y. C. Tang, in *Topics in Nuclear Physics II,* edited by T. T. S. Kuo and S. S. M. Wong, Lecture Notes in Physics Vol. 154 (Springer-Verlag, Berlin, 1981), p. 572.
[14]D. Baye, P.-H. Heenen, and M. Libert-Heinemann, Nucl. Phys. **A291**, 230 (1977).
[15]A. B. Volkov, Nucl. Phys. **74**, 33 (1965).
[16]F. Ajzenberg-Selove, Nucl. Phys. **A506**, 1 (1990).
[17]P. Descouvemont and M. Vincke, Phys. Rev. A **42**, 3835 (1990).
[18]D. Baye and P. Descouvemont, Nucl. Phys. **A507**, 497 (1990).
[19]D. Baye, P.-H. Heenen, and M. Libert-Heinemann, Nucl. Phys. **A308**, 229 (1978).
[20]P. Swan, Proc. R. Soc. London **A228**, 10 (1955).
[21]H. Walliser, T. Fliessbach, and Y. C. Tang, Nucl. Phys. **A437**, 367 (1985).
[22]F. C. Barker and T. Kajino (unpublished).